This paper appeared in *Prog. Photovolt: Res. Appl;* 2003; **11**: 1-13

Metal fingers on grain boundaries in multicrystalline silicon solar cells

Rita Ebner[a] [1], Michael Radike[a], Viktor Schlosser[b] and Johann Summhammer[a] [2]
[a] Atominstitut of the Austrian Universities
Stadionallee 2, A-1020 Wien, Austria
[b] Institute of Material Physics
University of Vienna, A-1090 Wien, Austria

Abstract: We have developed a method of applying a net-like finger grid to the front side of multicrystalline (mc) silicon solar cells, which lies mainly on the grain boundaries (Grain Boundary Oriented Finger grid, GBOF grid). This net has no busbars. It is drawn by a plotter using screen printing paste dispensed through a fine tube. The power output of cells contacted in this manner has been tested in a statistical study of pairs and triplets of cells of size 100x100 mm^2 (Bayer) and 103x103 mm^2 (Eurosolare). In the pairs-study pairs of neighbouring wafers of the original ingot were processed into solar cells. One wafer received a GBOF-grid, the other got the same grid rotated by 90 degrees and so had little coverage of grain boundaries. In the study of triplets the third wafer of each triplet was equipped with a standard H-pattern of the same shading as the GBOF-grid. In the pairs study we find that under approximately standard conditions there is an 89% chance that the GBOF-grid increases power output over cells with identical but 90 degrees rotated grid, the most probable increase being by 2.6%. The triplets study shows that there is an 87% chance that the GBOF-grid increases power output over cells with standard H-pattern, the most probable increase being by 2.5%.

1. Introduction

The grain boundaries in multi-crystalline silicon solar cells are regions of enhanced recombination for minority carriers and pose potential barriers to majority carriers [1],[2],[3],[4]. Together with the higher concentration of in-grain defects in multi-crystalline silicon, this is the main reason for lower conversion efficiency of multi- compared to mono-crystalline silicon solar cells. The usual way of countering these effects is to passivate the grain boundaries with hydrogen atoms [5],[6], often in combination with surface passivation [7], and to try to getter impurities during the cell production process (e.g. [8]). In the present work another method has been investigated, which may also be applied in addition to the existing methods: The front metal grid of the solar cell has been designed such that it mainly follows the grain boundaries. Theoretically, this entails some beneficial effects:

- The shading due to the metal lines is over areas of short lifetime, thereby exposing more long lifetime area to sun light. This should increase the short circuit current.
- Since 'dead' area is used, the metal lines can be thicker, which reduces the series resistance.

[1] Email: rita.ebner@ati.ac.at
[2] Author checking the proofs.
Email: summhammer@ati.ac.at
Tel. ++43 - 1 - 58801 - 14127
Fax. ++43 - 1 - 58801 -14199
Homepage: www.ati.ac.at/~summweb

- The electrons in the n-doped emitter drifting to the metal lines do not have to cross the potential barriers at the grain boundaries. This, too, reduces the series resistance.

A quantitative theoretical investigation of these effects is difficult, although a two-dimensional simulation of the effect of shading the grain boundary in a model of a silicon solar cell consisting of two adjacent grains has been presented in [9]. But it is worth looking at the possible gain in current. Assume a multicrystalline cell with columnar grains of a mean size of $5\times5mm^2$ and a diffusion length of minority carriers in the bulk of $100\mu m$. Light striking the surface within about one diffusion length of a grain boundary will produce little or no current, rendering about 4% of the area of the cell as 'dead'. Therefore, a corresponding increase in short circuit current can be expected, if this area were used for metallization instead of 'good' in-grain area. Still, adverse effects of grain boundary contacting are conceivable. Phosphorous diffusion down grain boundaries is very fast, which can provide shunting paths and at the same time result in lower doping density of the emitter at a grain boundary [10]. This could increase the contact resistance. However, in the experiments, the overall effect of grain boundary contacting is positive. We find a statistical improvement of short circuit current, fill factor and power output.

2. Experiments

2.1 Layout of the study

The study was done on a series of pairs of solar cells made from adjacent wafers of the original ingot, and then on a series of triplets, similarly obtained from neighbouring wafers. It built on earlier work on much smaller cells [11] and on narrow strips of a cell divided by one grain boundary [12]. Further motivation came from the results of another group, who applied grain boundary contacts in addition to the usual geometric contact pattern [13].

The pairs study was done on Baysix $100\times100mm^2$ wafers of about $270\mu m$ thickness and on Eurosolare $103\times103mm^2$ wafers of about $340\mu m$ thickness, both boron doped between 0.5 and 2.0 $\Omega.cm$. The triplets study was done only on Baysix wafers. In the pairs study one wafer of each pair received the GBOF-grid and the other got the same grid but rotated by 90^o before application. From now on we shall call solar cells with the former grid 'ON-cells' and with the latter grid 'OFF-cells'. Since the two wafers had almost identical grain structure, it could be expected that any difference in performance of the solar cells would be largely due to the way the front metal grid was placed relative to the grain boundaries. In the triplets study the additional solar cell of each triplet was equipped with a standard H-grid consisting of parallel fingers and two busbars. We shall call these cells 'STD-cells'. But care was taken that the shading of this grid was the same as that of the GBOF grid. This was done by first determining the optimal number of fingers for the STD-cell, and then using the effective shading of this grid to fix the parameters for calculation of the GBOF-grid. The purpose of the triplets study was to see whether the GBOF-grid, when rotated by 90^o, so that it would not follow the grain boundaries, showed any difference in its electrical parameters compared to the standard H-grid, which seems to be optimal with respect to minimizing optical and electrical losses. Since in both cases grain boundaries would be covered only accidentally, the difference should be mainly attributable to different series resistance losses. In this paper we present the results of about 140 cells made under the pairs study and of about 80 cells made under the triplets study. Roughly 10% more cells were actually made.
In overview, the experiments were conducted in the following way:

a) Exploratory run

- Only a pairs study to optimize the GBOF grid layout.

b) Main run

- First part as a pairs study to bring out the pure effect of on-grain-boundary contacting.
- Second part as a triplets study to have a comparison between GBOF-grid and standard H-grid.

2.2 Solar cell preparation and characterisation

2.2.1 Laboratory process

The solar cells were made in batches of typically 20 pieces because the quartz boat of the diffusion furnace was limited to 25 pieces and 2 to 3 wafers served as buffers against the gas draft at either end. The following process and characterisations were used:

1. Saw damage removal and preferential etching to facilitate optical grain boundary detection, both in hot NaOH. (In some batches only saw damage removal using HF/HNO_3.)
2. On some samples: Determination of minority carrier lifetime by the photo conductance decay method.
3. pn-junction formation in $POCl_3$ atmosphere at 840^o C for 75 minutes.
4. Measurement of n-emitter sheet resistance at 9 points on each side of wafer.
5. Full backside metalization with screen printed Al/Ag paste.
6. Drying of paste at 160^oC, burn-off of flammables at 450^oC for $60s$ and sintering at 710^oC for $60s$.
7. Optical scanning of front side of wafer in flat bed scanner to obtain a 1-byte per pixel grey scale image at 508 dpi ($50\mu m \times 50\mu m$ per pixel).
8. For some batches of triplets study: Calculation of optimal number of fingers for standard H-grid according to emitter sheet resistance of the particular cell and calculation of corresponding number of lines of GBOF-grid, so that both kinds of grid would have the same shading.
9. Calculation of the lay out of the GBOF-grid using grey scale image of the respective wafer as input.
10. Drawing of front grid with Ag screen printing paste with a $250\mu m$ dispensing tube using an x-y-plotter of $25\mu m$ step increment.
11. Drying of paste at 160^oC, burn-off of flammables at 450^oC for $60s$ and sintering at 710^oC for $60s$.
12. Mechanical abrasion of parasitic junction at the edges.
13. Current-voltage characterisation of cell, in the dark and under illumination.

The cells received no anti-reflection coating and no passivation of the grain boundaries.

The sheet resistance of the emitter ranged between 25 and $35\Omega/\Box$, going as high as $45\Omega/\Box$ at the first and last wafer. There was a typical profile in each batch, which showed low resistivity in the middle and higher resistivity at both ends of the boat. In those batches, in which the front metal grid was not optimised for each pair or triplet, a mean value of 30Ω was assumed. It may have happened that for a given pair or triplet the emitter sheet resistance differed by as much as 20% between the wafers, but since there was a random variation as to which wafer got which kind of front pattern, any systematic influence on the performance of the cells with the different grids can safely be assumed to have canceled out.

The paste used for the back side was Ferro FX33-130, and the one for the front side was Ferro 3347 Ag Conductrox. All three kinds of patterns on the front were written with a dispensing tube of $250\mu m$. After sintering the typical line thickness was $350\mu m$. The specific line resistance, determined on separate wafers without n-doping, was approximately $30m\Omega/cm$. The contact resistances were also established on separate wafers having an n-emitter just as the actual solar cells. Typical values were 11 to 12 $m\Omega cm^2$. The two busbars on the STD-cells were each written as four closely spaced fingers. A triplet of wafers is shown in Fig.1. Note that their grain boundary structure is very similar, because they were neighbours in the ingot. Fig.1a shows the ON-cell, Fig.1b the OFF-cell and Fig.1c the STD-cell.

2.2.2 The GBOF grid

Some details on the calculation of the layout of the GBOF-grid have already been given elsewhere, so that a summary can suffice here [14]. First, a theoretical grid is assumed, consisting of a certain number of equidistant horizontal lines. Between these, short pieces of vertical lines are placed. The number of horizontal, respectively vertical, lines can be chosen according to the optimum value calculated from the emitter sheet resistance, the finger line and contact resistivities and total shading, as well as the light generated current per unit area. Usually an emitter sheet resistance of $30\Omega/\Box$ was assumed, and a light-generated current density of about $20mA/cm^2$, as previously found in similarly processed cells tested under standard conditions. Then this grid is put over the grey scale image of the wafer and the lines are bent and twisted within adjustable limits, so that they come to lie over grain boundaries as much as possible. The resulting number of vertical lines between any two neighbouring horizontal lines is then not always the same, not even on the same cell. Grain boundaries are detected as abrupt changes of brightness in the grey scale image of the front side of the wafers. The image is obtained at $50\mu m$ resolution (higher resolution would add noise because surface steps from etching in NaOH become noticeable) but plotted with $25\mu m$ positioning accuracy of the dispensing tube. Both values are well below the final thickness of the lines to be drawn. The writing speed of the lines was between 0.5 and $1mm/s$. The whole process from scanning the image to writing the GBOF grid on the wafer was automated, except for positioning the wafer on marker points on the x-y-table before writing.

The percentage of the wafer front surface which is shaded by the grid lines is determined by optically scanning the finished solar cells in the photographic scanner and determining the fraction of pixels whose brightness is above a certain value. This is possible, because the reflectivity of the fired silver paste is much higher than that of most grains. The actual shading of the front grid of STD-cells was also determined in this manner. It turned out that the theoretically expected shading and the actual shading were in very good agreement (sec. 3.2.1).

The GBOF grid had to be constrained to a certain mesh density in order to avoid undue losses in the emitter sheet, it could not always follow grain boundaries. The fraction of line length that really lay over grain boundaries was determined by checking, which of the pixels in the theoretical image of the GBOF-grid coincided with those pixels in the grey scale image of the wafer which were identified as grain boundary points because they were on a line of sudden change of brightness. It turned out that the fraction of grid length on grain boundaries was typically 64 - 75% for ON-cells, whereas it was only 17 - 31% for OFF-cells. These values contain some noise, so that they are an overestimate, but the difference is quite reliable. The 'on grain boundary' fraction of the GBOF-grid was thus really significant, although it can certainly be pushed closer to 100%. Actual values are given in the tables below. (In the first series of cells, produced as an exploratory run whose results are shown in Table I, the GBOF-grid calculation software was less efficient, and the 'on grain boundary'-fraction was correspondingly lower. See caption of Table I.)

2.2.3 Characterisation

The characterisation of the finished solar cells was done by current-voltage measurements in the dark and under illumination. The current of ON-cells and of OFF-cells was tapped at four points close to the corners, noticeable in Figs.1a and 1b, and of STD-cells it was tapped at both ends of both bus bars. The voltage was taken at a fifth point in all three kinds of cells. At the back the whole area was contacted for current, except for a small region in the middle which served as contact point for voltage measurement. The illumination was provided by two 500 watts quartz lamps whose distance to the wafer was set such that a known reference cell gave the same short circuit current as under a sunlight simulator of AM1.5 spectrum. In some cases the intensity was reduced to 75%, 50% and 25%, respectively. The cells were kept at room temperature (19 - 22^{o}C).

3. Results

3.1 Exploratory run

In the exploratory run five batches of 20 cells each were produced from Baysix wafers (size 100×100 mm^2). It was conducted as a pairs study and served to find out the proper density of lines. Therefore, cells with an average spacing of the horizontal and vertical lines of 4mm, 6mm and 8mm, respectively, were prepared. The grain-boundary tracing software was not yet sufficiently developed, in that the horizontal lines tended to have a lower percentage of length on grain boundaries than did the vertical lines. But we present the results here, because they gave a first indication that the ON-cells tended to have a higher fill factor than the OFF-cells, which motivated the further investigations. In particular, it was found that if one looks at all cells with a fill factor larger than 50%, the OFF-cells tended to be slightly superior to the ON-cells. However, if only cells with a fill factor larger than 60% are included, the ON-cells were superior. This can be seen in the column P_r in Table I, which gives the ratio of maximum power outputs of ON-cells to OFF-cells.

3.2 Main run

3.2.1 Overall results

The results of the main run are shown in Table II. It consisted of a pairs study (groups A and B) and of a triplets study (groups C, D and E), for which altogether around 180 cells were made.

Some cells broke and in some cells one or several parameters were far from the mean value of the respective group, so that they were easily detected as faulty and were also not included in the results compiled in the table. Therefore some pairs or triplets were not complete, as can be inferred from the column 'cells'. Only in group B all cells turned out of good quality, so that it is comprised of ten true pairs. Group B were Eurosolare wafers, all others were Baysix wafers. Wafers of groups A, B, C, D were damage etched and surface structured in NaOH. Wafers of group E were only damage etched in HF/HNO_3. For groups A, B, C the optimal coverage of the front grid was calculated from the mean value of the sheet resistance of the emitters of the whole group. For groups D and E it was calculated from the mean value of the sheet resistance of the emitters of each triplet separately. (For a few triplets, which were made from wafers positioned close to the ends of the boat in the diffusion furnace, this could mean a difference of around 20% between the three wafers.) Since the pattern tracing software was improved with respect to the exploratory run, the percentage of line length of the front grid of ON-cells which followed grain boundaries was higher. On average, in the ON-cells the front grid ran over grain boundaries for 68.7% of its length, while in the OFF-cells it was only 23.3%, giving a difference of 45.4%, as can be obtained from the column 'GB'.

The shading caused by the front grid was typically between 11.0% and 11.8% for cells of groups A and B. For group C it was almost always 11.0% ($\pm$0.2%), both for ON-cells and OFF-cells on the one hand and STD-cells on the other. The optimization procedure employed for groups D and E led to a shading of mostly 8.9% for cells of group D (only two cells with higher sheet resistance were covered to 9.6% and 10.5%, respectively), and to a coverage between 7.6% and 8.1% for cells of group E. The difference in front grid shading between ON- or OFF-cells and STD-cells for any triplet in these groups was usually no more than 0.2% of the cell's area.

The results of the main run are also displayed in Figures 2 to 4, where the value of the respective quantity of each individual cell is shown as a horizontal bar. Mean values of the group are highlighted as wider horizontal bars.

For some wafers of groups A, B, D and E the lifetime of the minority carriers in the base was determined after etching back the phosphorous diffused layer. The photo conductance decay method was applied [15]. The lifetimes were between 10 and 80μs, with a predominance of values around 40μs, the typical uncertainty being around $\pm$10μs. The value of 80μs was attained with a wafer from a batch of group A, that batch showing a tendency to higher short circuit current (Fig.2). However, the overall statistics were not yet sufficient to discern a clear relation between lifetime and difference in power output of ON-cells versus OFF-cells.

A remark must be made concerning the fill factor, Fig.4. For all cells it is lower, on average, than possible with the screen printing pastes used. This is due to the firing profiles, which led to non-optimal contact resistances. But since the contact area in the cells to be compared was virtually the same, the conclusions to be drawn from the results are not affected [16].

A closer look at table II and at figures 2 to 4 reveals that the ON-cells exhibit the higher mean values of open circuit voltage[3] (except in group E), the higher mean values of short circuit current (except in group C), and the higher mean values of the maximum power output (true for all groups). This is emphasized in the column 'P_r' in table II, which gives the values of maximum power as a percentage of maximum power of OFF-cells: For the ON-cells this value is always above 100%.

The effect of the grain boundary contacting as such can be seen by comparing the ON-cells to the OFF-cells. The weighted mean of the short circuit current density of ON-cells from all

[3]In multicrystalline cells U_{oc} is not only determined by the diode saturation current of the individual crystallites, but also by the potential barriers between them, which can be affected by the GBOF grid.

five groups is $19.258 mA/cm^2$, while for the OFF-cells it is $19.073 mA/cm^2$. This corresponds to an increase of short circuit current density of ON-cells versus OFF-cells of 0.97%. It seems to confirm our original motivation that ON-cells expose more high-lifetime area to the incident light and have lower series resistance losses. This is also reflected in the mean of the maximum power of ON-cells and OFF-cells from all five groups. Taking again the weighted mean, the average ON-cell yielded $7.149 mW/cm^2$, whereas the average OFF-cell yielded $6.965 mW/cm^2$. Thus, on average, the ON-cells give 2.63% more power than the OFF-cells at approximately standard conditions. It is also instructive to look at the pairs study and at the triplets study separately, because they had slightly different processing conditions as mentioned above. Taking only groups A and B, the ON-cells give 3.71% more power than the OFF-cells. When taking the groups C, D and E, the ON-cells give 1.98% more power than the OFF-cells. (Concerning the difference between Baysix and Eurosolare wafers, the overall data of groups A and B in table II could be interpreted to imply that our whole processing sequence — established first on Eurosolare wafers some time before the present study — was better suited to the Eurosolare wafers.)

The relative merits of the grain boundary contacting scheme over the standard scheme can be assessed by comparing the ON-cells and the STD-cells of the triplets study. Taking the weighted mean of ON-cells of groups C, D and E gives an average maximum output power density of $6.882 mW/cm^2$ and for the STD-cells this gives $6.714 mW/cm^2$. This is an increase of power output density of 2.50% of ON-cells over the STD-cells. For the OFF-cells one obtains $6.749 mW/cm^2$, which is 0.52% above the STD-cells. This latter difference shows that, when going from the standard H-grid of the STD-cells to the net-like grid of the OFF-cells, while aiming at having the same shading for both, the power output of the cells changes very little.

The busbars in the STD-cells had a specific line resistance of about $7.5 m\Omega/cm$ and were not reinforced by additional tabs for the measurements. But since the current was extracted at both ends of a busbar the resistive losses were estimated to be at most $12 mW$. For the same current, similar industrial cells with tabbed busbars of a specific line resistance of about $1.5 m\Omega/cm$ and current drawn from *only one end* would show about $9 mW$ loss in both busbars. Our general finding that the ON-cells outperform the STD-cells would therefore not be affected, if the STD-cells had been tested with tabs and only one-sided current extraction.

For commercial applications of grain boundary contacting it is important to have statistical confidence levels for our results. These are calculated from the posterior probability distribution of the mean output power of the cells, assuming that each of the groups A to E represents a sample from a corresponding large scale production with a characteristic gaussian distribution of the output power of the cells. The mean power P_p of the cells from such a production can be estimated as [17]

$$P_p = P_s \pm \sqrt{\frac{\sigma_s^2}{N}}, \tag{1}$$

where P_s, σ_s and N are the mean power, the standard deviation, and the number of cells of the sample, respectively. Then we can obtain the overlap of the gaussian distributions of the estimated mean power of the ON-cells, of the OFF-cells and of the STD-cells, and thereby make a statement how confident we can be that in a large scale production one kind of cell would produce more power than another. The gaussians for the overall mean power of groups A to E of ON-cells and of OFF-cells are shown in Fig.5. From these we deduce that we can be 89% confident that the ON-cells will give more power than the OFF-cells, and that the most likely increase in power output of the ON-cells over the OFF-cells is 2.63%, as quoted

above. Also note that the distribution for the ON-cells is narrower than for the OFF-cells. This characteristic has also been found for the short circuit current, the fill factor and the open circuit voltage, suggesting that grain boundary contacting can lead to more even production results. A similar calculation for the ON-cells and the STD-cells of the triplets study (groups C to E) shows that we can be 87% confident that the ON-cells produce more power than the STD-cells, and that the most likely increase in power output of the ON-cells over the STD-cells is 2.50%.

3.2.2 Different illumination levels

For the cells of group A the current-voltage curves were also recorded for lower illumination levels. For this purpose a high resolution photographic film with fine black lines was placed between the lamps and the solar cell. One film had a nominal transmission of 50% and the other of 25%. The ON-cells produced higher average power than the OFF-cells at all illumination levels, but the relative difference between them decreases as the illumination goes down.

The cells of group A consisted of two different batches with somewhat different values of the short circuit currents[4], as can be seen in Fig.3. But both batches showed this behaviour. The mean values of the whole group A are as follows. At an illumination intensity of 25% of our approximate standard conditions, the ON-cells produced 0.14% more power than the OFF-cells, at an intensity of 50% it was 1.51% more, and at 100% it was 2.60% more (as already listed in table II in column 'P_r').

The most likely explanation for this dependence on illumination intensity is the ON-cells' lower series resistance losses in the emitter and at the interface between emitter and metal grid. Since this grid is mainly along grain boundaries, electrons drifting in the emitter on the way to the metal grid have to cross potential barriers between different grains less often. And the higher doping at the grain boundaries might reduce the contact resistance. Note that, if the difference between ON-cells and OFF-cells were only that the former exposed more good grain area to the incident light than the latter, one would expect that the relative difference in power output should not depend on the intensity.

Measurements of power output under two different illumination levels were also made on six of the ten pairs of cells made from Eurosolare wafers (group B). These data were taken at another test station supplying $1000 W/m^2$ with approximately AM1 spectrum, which were then reduced to about 1/8 ($127 W/m^2$). The results confirmed what was found for the cells of group A, namely that the power output of the ON-cells is higher than that of the OFF-cells for both illumination levels, but that the relative difference decreases at the lower intensity.

Considering that the cells had no antireflection coating permits to draw an interesting conclusion from these findings: When more current is generated due to better coupling of light into the cells, the ON-cells might outperform the OFF-cells and the standard cells by a somewhat larger percentage than observed so far.

3.2.3 Temperature dependence of power output

For the six pairs of cells from group B just mentioned current-voltage curves under AM1-conditions were also recorded as a function of temperature in the range between 300 and 330 K. The general behaviour followed the theoretical expectation that the short circuit current increases with temperature, but open circuit voltage, fill factor and maximum power output

[4]The cause of this difference seems to be different humidity in the laboratory during the phosphorous diffusion process, leading to different emitter sheet resistances at otherwise identical process conditions.

decrease. However, it turned out that the decrease of fill factor and consequently of power output happened noticeably faster for the ON-cells than for the OFF-cells.

For the temperature range of interest one can define a linear temperature coefficient for the fill factor as

$$\alpha_{FF} = \frac{\left(\frac{\Delta FF}{\Delta T}\right)}{FF_{(300)}}, \tag{2}$$

where ΔFF is the change in fill factor over the temperature range ΔT, and $FF_{(300)}$ is the fill factor at 300 K. The mean value of α_{FF} for the six ON-cells was -0.36%/K, while for the OFF-cells it was only -0.29%/K.

When one defines a linear temperature coefficient for the maximum power output as

$$\alpha_{MP} = \frac{\left(\frac{\Delta P_m}{\Delta T}\right)}{P_{m(300)}}, \tag{3}$$

where ΔP_m is the difference of a cell's maximum power over the temperature range ΔT and $P_{m(300)}$ is the maximum power output at 300 K, one obtains a similar result. For the ON-cells one had $\alpha_{MP} \approx -0.79\%/K$ and for the OFF-cells $\alpha_{MP} \approx -0.68\%/K$.

An explanation for this faster decrease of power output with increase of temperature for ON-cells relative to the OFF-cells could be found in the lower series resistance of the ON-cells. In the single diode model the current-voltage relation of the illuminated solar cell is given by

$$I = -I_L + I_0 \left[e^{-\frac{q(V-IR_S)}{nk_BT}} - 1 \right] + G_{SH}(V - IR_S), \tag{4}$$

where I is the external current, V is the external voltage, I_L is the light-generated current, I_0 is an effective diode current due to saturation and recombination, n is the ideality factor (typically 2 in the fits to the I-V curves), k_B is Boltzmann's constant, R_S is the series resistance and G_{SH} is the shunt conductance. The diode current I_0 is itself temperature dependent via an activation law. When extracting from this equation the theoretical linear temperature coefficient of the maximum power output, α_{MP}, for realistic values of R_S and G_{SH}, one finds that α_{MP} does indeed become more negative with decreasing series resistance R_S. The advantage of lower series resistance of the ON-cells is thus a little diminished at higher temperatures. A more detailed treatment will be published elsewhere [18].

3.2.4 Series resistance

The indication for lower series resistance losses in ON-cells cannot be easily extracted from the dark and bright I-V-curves. It has been emphasized in [19] that the simple one-diode model of eq.(3), even when extended to a two-diode model, is not a physically correct description for large area cells and is often manifested in bad fits between model curve and data. It must be replaced by a more complex model of many small solar cells connected in parallel by finite resistances. However, data analysis by means of such a model requires current and voltage data at the maximum power point under many different illumination levels. Since such data are not available, another route has been chosen to assess the differences in resistive losses of the three kinds of cells.

At least two different contributions to the series resistance at the front side of the cells must be distinguished: An effective resistance R_e of the emitter sheet including its contact to the metal grid, and an effective resistance R_m of the metal grid up to the points of extraction of

power. One may expect that R_m should be the same for the ON-cells and the OFF-cells, while R_e should be different. On the other hand, the STD-cells should differ both in R_e and in R_m with respect to the ON-cells and to the OFF-cells.

In order to gain an understanding of these issues, two quantities were extracted from the dark and the bright I-V-curve of each cell:

- The 'series' resistance R_S as it appears in eq.(3), using a method proposed in [20]. It takes the voltage U_d of the dark curve under forward bias, when the absolute value of the current is the same as the short circuit current under illumination, I_{sc}. Because of the series resistance, U_d is smaller than the the open circuit voltage U_{oc} (except when the shunt resistance is very low), so that

$$R_S = \frac{U_d - U_{oc}}{I_{sc}}. \tag{5}$$

- The 'flank' resistance R_F, here defined as

$$R_F \equiv \frac{U_{oc} - U_{mp}}{I_{mp}}, \tag{6}$$

  where U_{mp} and I_{mp} are voltage and current density, respectively, at the maximum power point. R_F is an artificial quantity, which reflects the slope of the bright I-V-curve at voltages higher than U_{mp}. It can be an effective indicator for series resistance, because series resistance affects predominantly that part of the I-V-curve. But R_F does not vanish at zero series resistance. Therefore, noticeably different values of R_F for the different kinds of cells should be an even stronger indication of differences in series resistance.

Evaluation shows that R_S is lower for the STD-cells than for both the ON-cells and the OFF-cells, but a distinction between ON-cells and OFF-cells cannot be drawn. The lower value for the STD-cells is understandable, because the dark I-V-curve of the STD-cells has a stronger exponential rise, presumably because the busbars permit to distribute current efficiently to the whole metal grid. But since this happens under forward bias, most of the current flows from the n- to the p-side directly under the front metal grid, and there is little current flow in the emitter sheet. Therefore, R_S is a good indicator only for the metal grid component R_m of the total series resistance. The results suggest that this component is lower in the STD-cells than in the other cells. Table III summarizes the mean values for each kind of cell for all five groups. As in the previous tables, the numbers in brackets are the mean deviation from the mean, giving a measure of the width of the distribution of values for the specific kind of cells.

Evaluation of R_F shows in *all five groups* a lower value for the ON-cells than for the OFF-cells, while the STD-cells exhibit no clear tendency. Since R_F is based only on bright I-V-data, and since the metal grid component R_m should be the same for the ON-cells and the OFF-cells, it seems to represent a difference in the emitter sheet component R_e. Table IV summarizes these results.

Comparing the values of R_F for the ON-cells and the OFF-cells, one may conclude that the expected difference in series resistance of the emitter, and possibly of the contact between metal and emitter, does indeed exist. The GBOF-grid, in which a significant fraction of the total metal line length follows and covers grain boundaries, lowers the average ohmic resistance from any point in the emitter to the metal grid.

4. Conclusion

We have investigated the effect of designing the metal grid for current collection on the front side of multicrystalline silicon solar cells as a kind of net, whose lines follow grain boundaries wherever possible. There were no bus bars. The current was drawn from four points at the corners of the quadratic cells of industrial size ($100\times100mm^2$ and $103\times103mm^2$). The contact pattern was created automatically using the wafer's optical image as input and was plotted automatically with screen printing paste. It turned out that under approximately standard conditions cells with this kind of front contacts yield 2.5% more power, on average, than cells equipped with the standard H-pattern (two busbars and perpendicular fingers), when both patterns have the same shading and when the standard H-pattern is optimized for the given sheet resistance. The pure effect of having the current collecting lines follow the grain boundaries could be established by comparing these cells to those made from the immediate neighbours in the ingot, to which the same grid was applied, but rotated by 90 degrees, so that it covered grain boundaries only accidentally. Here, different batches showed that the on-grain-boundary contacted cells are superior in power output by 2.6%, on average. As the main cause for this difference the lower series resistance losses in the emitter sheet and possibly between emitter and metal of the new contacting scheme could be established, because the difference in power output became smaller with increasing temperature, as expected theoretically, and it also became smaller with lower illumination levels.

Future investigations will focus on identifying the electronically relevant grain boundaries by position resolved lifetime measurements, and on replacing the plotting of the contacts with screen printing paste by a galvanic process.

Acknowledgment

This work was made possible by a grant from the Austrian Science Foundation (Fonds zur Förderung der wissenschaftlichen Forschung), project number P14432.

References

[1] Seto JYW, The electrical properties of polycristalline silicon films, *Journal of Applied Physics* 1975; **46**: 5247-5254.

[2] Landsberg PT, Abrahams MS, Effects of surface states and of excitation barrier heights in a simple model of a grain boundary or surface, *Journal of Applied Physics* 1984; **55**: 4284-4293.

[3] Edmiston SA, Heiser G, Sproul AB, Green MA, Improved modeling of grain boundary recombination in bulk and p-n junction regions of polycrystalline silicon solar cells, *Journal of Applied Physics* 1996, **80**: 6783-6795.

[4] Weis T., Lipperheide R., Wille U., Systematic theoretical study of grain boundary effects in photovoltaic materials, *Conference proceedings, 2nd World Conference and Exhibition on Photovoltaic Solar Energy Conversion*, Vienna, 1998: 1438-1441.

[5] Lüdemann R, Hauser A, Schindler R, Hydrogen passivation of low- and high-quality mc-silicon for high-efficiency solar cells, *Conference proceedings, 2nd World Conference and Exhibition on Photovoltaic Solar Energy Conversion*, Vienna, 1998: 1638-1641.

[6] Elgamel HE, Vinckier C, Caymax M, Ghannam M, Poortmans J, De Schepper P, Nijs J, Mertens R, High efficiency multicrystalline silicon solar cells using hydrogen remote plasma passivation, *Conference proceedings, 12th EPVSEC*, Amsterdam, 1994: 724-727.

[7] Aberle AG, *Crystalline Silicon Solar Cells, Advanced Surface Passivation and Analysis*, Bloxham and Chambers Printery, Rhodes NSW, Australia, 1999.

[8] Stocks M, Cuevas A, Blakers A, Minority carrier lifetimes of multicrystalline silicon during solar cell processing, *Conference proceedings, 14th EPVSEC*, Barcelona, 1997: 770-773.

[9] Mittelstaedt L, Metz A, Hezel R, Presentation HL2.9 at spring meeting of solid state physics section of German Physical Society, Münster, 22-26 March 1999; unpublished.

[10] Green MA, *Solar Cells* (Prentice Hall, New Jersey, 1982) p.188.

[11] Summhammer J, Schlosser V, Investigation of a novel front contact grid on poly silicon solar cells, *Conference proceedings, 12th EPVSEC*, Amsterdam, 1994: 734-736.

[12] Schlosser V, Summhammer J, A study of the charge transport across grain boundaries in polycrystalline silicon solar cells with a front contact along the grain boundaries, *Conference proceedings, 14th EPVSEC*, Barcelona, 1997: 716-719.

[13] Kim HW, Lim DG, Lee SE, Kim SS, Yi J, Poly-Si Solar Cells with an Electrode along Grain Boundaries, *Conference proceedings, 2nd World Conference and Exhibition on Photovoltaic Solar Energy Conversion*, Vienna, 1998: 1728-1731.

[14] Radike M, Summhammer J, Novel process of grain boundary metallisation on mc Si solar cells, *Solar Energy Materials and Solar Cells* 2001: **65**, 303-309.

[15] Sinton RA, Cuevas A, Contactless Determination of Current-Voltage Characteristics and Minority-Carrier Lifetime in Semiconductors from Quasi-Steady State Photoconductance Data, *Applied Physics Letters*, 1996: **69**, 2510-2512.

[16] Latest tests with galvanic deposition of the front contacts over the grain boundaries have resulted in much better fill factors: www.ati.ac.at/~summweb, section *Research*.

[17] Spiegel MR, *Theory and Problems of Statistics*, (Schaum's Outline Series in Mathematics, McGraw-Hill Book Company, 1961) p.167 ff.

[18] Schlosser V, to be published: Temperature dependence of performance and local heating of crystalline silicon solar cells with GBOF-grid.

[19] Fischer B, Fath P, Bucher E, Evaluation of solar cell J(V)-measurements with a distributed series resistance model, *Conference proceedings, 16th EPVSEC*, Glasgow, 2000: Paper VA1.40. (File D340.pdf on CD version.)

[20] Goetzberger A, Voß B, Knobloch J, *Sonnenenergie: Photovoltaik*, B. G. Teubner, Stuttgart, 1997, p.228.

Table I: Results of exploratory run. Average values of power output per unit area and of fill factor. The numbers in brackets are mean deviations from the average. The upper half includes all cells with a fill factor above 50%, the lower half includes only those cells whose fill factor was above 60%. The percentage of the total line length of the front grid which was along grain boundaries was between 43% and 63% for ON-cells and between 10% and 24% for OFF-cells. The mean difference of these values between ON-cells and OFF-cells was 36.5%.
Column labels:
Spacing...distance of lines of theoretical grid from which grid calculation starts
Grid...'ON': cells with GBOF grid, 'OFF': cells with GBOF grid rotated by 90 degrees
Cells...number of cells included in the analysis
P_m...maximum output power density under approximately standard conditions
P_r...maximum output power density relative to maximum output power density of cells with 'OFF'-grid
FF...fill factor

Spacing	Grid	Cells	$P_m[mW/cm^2]$	P_r (%)	$\mathrm{FF}_{(>50)}$(%)
4mm	ON	17	6.534 (.491)	**99.71**	63.0 (3.1)
4mm	OFF	15	6.553 (.476)	100.00	63.4 (2.7)
6mm	ON	4	6.560 (.635)	**95.82**	62.1 (5.3)
6mm	OFF	5	6.846 (.093)	100.00	64.2 (1.6)
8mm	ON	6	6.320 (.616)	**98.24**	58.2 (4.7)
8mm	OFF	4	6.433 (.451)	100.00	58.6 (3.1)
					$\mathrm{FF}_{(>60)}$(%)
4mm	ON	13	6.781 (.276)	**101.89**	64.8 (1.8)
4mm	OFF	14	6.655 (.401)	100.00	64.2 (2.1)
6mm	ON	3	6.983 (.196)	**102.00**	65.6 (0.9)
6mm	OFF	5	6.846 (.093)	100.00	64.2 (1.6)
8mm	ON	3	6.903 (.230)	**101.20**	62.3 (0.8)
8mm	OFF	2	6.821 (.151)	100.00	61.1 (0.8)

Table II: Results of main run. It shows the mean values of characteristic parameters of the different types of cells of the pairs study (groups A and B) and of the triplets study (groups C, D and E). The numbers in brackets are the mean deviations (not the standard deviations, because that would be too sensitive to outliers in our small statistics). Group B are Eurosolare wafers, the others are Baysix wafers. Cells with a fill factor below 50% were not included.
Column labels (if not specified, same as in Table I):
Group...group of cells produced in identical fashion (could consist of several subsequent batches in the diffusion furnace)
Grid...'ON': cells with GBOF grid, 'OFF': cells with GBOF grid rotated by 90 degrees, 'STD': cells with standard H-pattern grid
U_{oc}...open circuit voltage
I_{sc}...short circuit current density
GB...percentage of the total line length of the front grid that lies over grain boundaries

Group	Grid	Cells	$U_{oc}[mV]$	$I_{sc}[mA/cm^2]$	$P_m[mW/cm^2]$	P_r (%)	$FF_{>50}$(%)	GB(%)
A	ON	14	566.7 (2.9)	19.15 (0.97)	7.065 (0.593)	**102.60**	65.0 (3.4)	67.7 (3.7)
A	OFF	15	565.5 (3.9)	19.15 (1.04)	6.886 (0.697)	100.00	63.3 (4.3)	21.9 (3.8)
B	ON	10	569.1 (3.9)	20.23 (0.34)	7.902 (0.205)	**104.72**	68.7 (2.1)	69.9 (1.2)
B	OFF	10	567.9 (2.5)	20.03 (0.30)	7.545 (0.452)	100.00	66.3 (4.5)	30.5 (2.4)
C	ON	14	550.9 (3.1)	18.42 (0.42)	6.689 (0.397)	**102.29**	66.0 (4.0)	64.9 (1.2)
C	OFF	13	548.8 (3.0)	18.01 (0.51)	6.539 (0.508)	100.00	66.1 (4.1)	16.9 (1.4)
C	STD	15	548.2 (5.0)	18.46 (0.20)	6.661 (0.562)	101.87	65.8 (5.0)	-
D	ON	6	554.3 (4.0)	19.03 (0.29)	6.848 (0.245)	**106.12**	64.9 (1.5)	70.4 (4.6)
D	OFF	4	551.4 (2.8)	18.61 (0.42)	6.453 (0.714)	100.00	62.7 (6.0)	24.7 (4.2)
D	STD	6	533.1 (14.1)	18.80 (0.36)	6.527 (0.434)	101.15	65.0 (2.6)	-
E	ON	7	554.7 (3.8)	19.66 (0.33)	7.299 (0.212)	**100.84**	66.9 (1.5)	75.0 (1.5)
E	OFF	8	555.2 (3.2)	19.43 (0.46)	7.238 (0.173)	100.00	67.1 (1.2)	26.6 (4.3)
E	STD	7	552.5 (3.1)	19.52 (0.40)	6.988 (0.204)	96.55	64.8 (1.9)	-

Table III:

	R_S [Ωcm^2]		
Group	ON-cells	OFF-cells	STD-cells
A	7.624 (0.849)	7.976 (0.536)	—
B	7.922 (0.197)	7.912 (0.282)	—
C	9.032 (0.612)	8.894 (0.819)	7.420 (0.885)
D	7.612 (0.601)	7.805 (0.933)	6.707 (1.030)
E	7.090 (0.272)	7.544 (0.505)	7.012 (0.560)

Table IV:

	R_F [Ωcm^2]		
Group	ON-cells	OFF-cells	STD-cells
A	8.281 (1.149)	8.934 (1.607)	—
B	6.916 (0.571)	7.593 (1.229)	—
C	8.242 (1.242)	8.292 (1.368)	8.256 (1.424)
D	8.111 (0.385)	9.094 (2.058)	7.804 (0.622)
E	7.279 (0.470)	7.371 (0.282)	8.082 (0.487)

Figure Captions

Fig.1: Three neighbouring wafers made into the three different cells of a triplet: (a) The front contact grid is laid out as a grain boundary oriented finger grid (GBOF-grid), which is mainly over grain boundaries (ON-cell). (b) The same grid, but rotated by 90 degrees before it is applied to the cell, so that only little grain boundary area is covered (OFF-cell). (c) Cell with a conventional H-pattern grid (STD-cell).

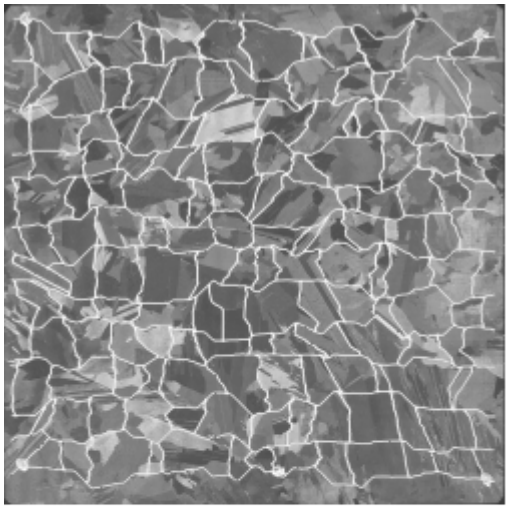

(a)

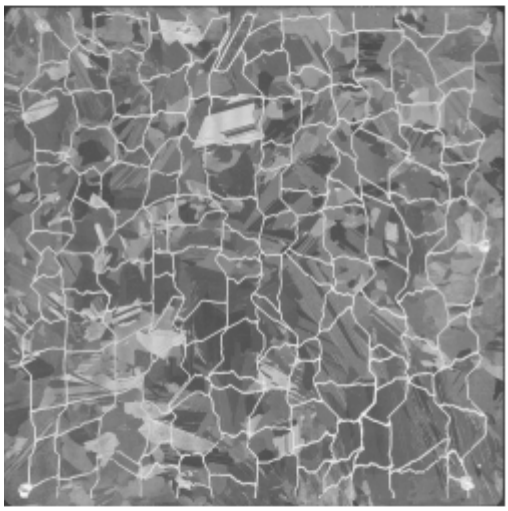

(b)

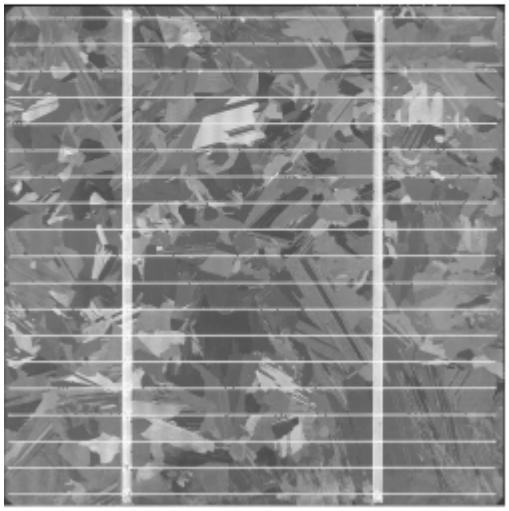

(c)

Figure 1:

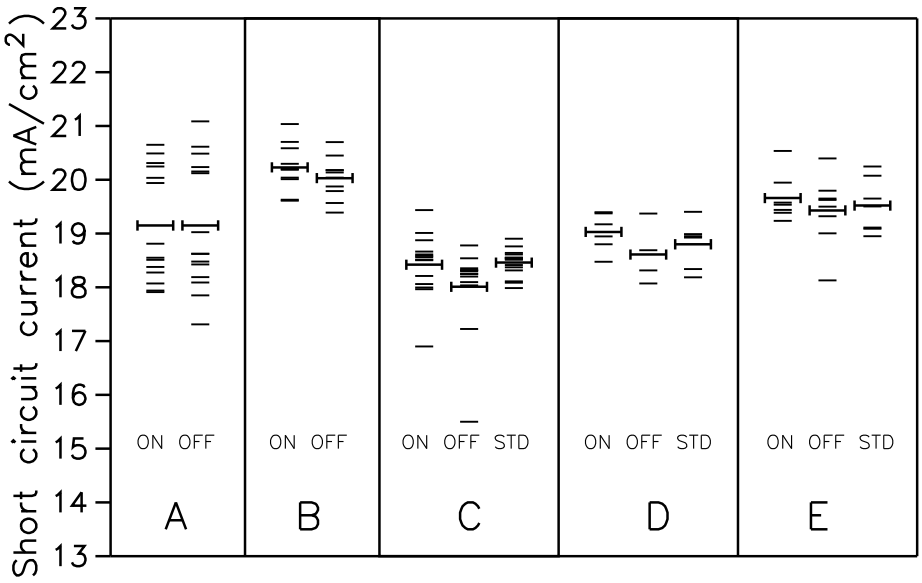

Figure 2: Short circuit currents of all cells of main run, and mean values of the different kinds of cells of the different groups.

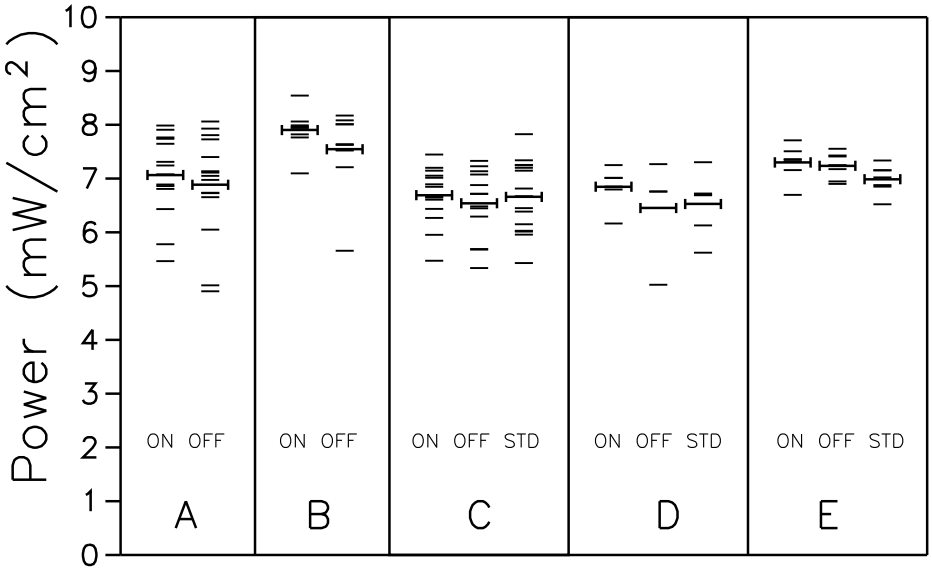

Figure 3: Maximum power of all cells of main run and average values.

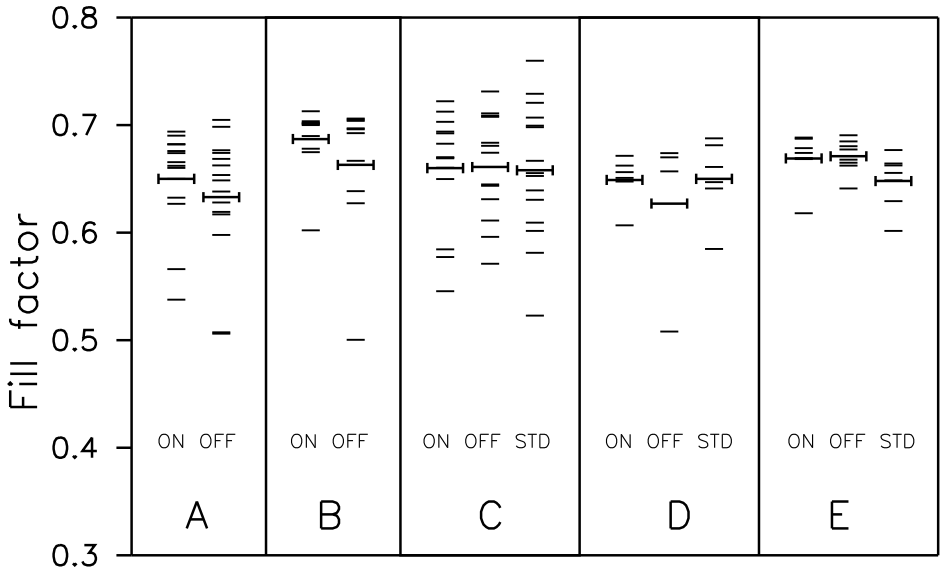

Figure 4: Fill factor of all cells of main run and average values.

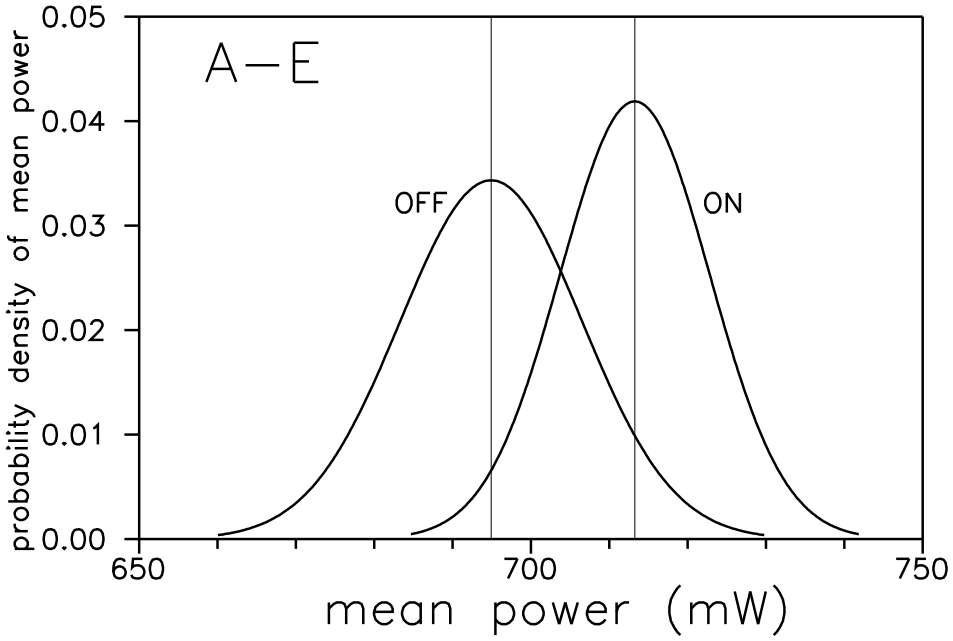

Figure 5: Inferred gaussian probability distributions of mean power output of ON-cells and OFF-cells of *all* groups of main run (groups A to E). It shows a most likely increase of power output of ON-cells against OFF-cells by 2.63% (7.133 against $6.949 mW/cm^2$).